Published as: *Immunity*. 2011 August 26; 35(2): 208–222.

T Cell Receptor Internalization from the Immunological Synapse is Mediated by TC21 and RhoG GTPase-Dependent Phagocytosis

Nuria Martínez-Martin[1], **Elena Fernández-Arenas**[1], **Saso Cemerski**[2], **Pilar Delgado**[1], **Martin Turner**[3], **John Heuser**[4], **Darrell J. Irvine**[5], **Bonnie Huang**[5], **Xosé R. Bustelo**[6], **Andrey Shaw**[2], and **Balbino Alarcón**[1,7]

[1]Centro de Biologia Molecular Severo Ochoa, CSIC-UAM, 28049 Madrid, Spain

[2]Department of Pathology and Immunology, Washington University School of Medicine, Saint Louis, MO 63110, USA

[3]Laboratory of Lymphocyte Signalling and Development, The Babraham Institute, Cambridge, CB22 3AT, UK

[4]Department of Cell Biology, Washington University School of Medicine, Saint Louis, MO 63110, USA

[5]Department of Biological Engineering, Massachusetts Institute of Technology, Cambridge, MA 02139, USA

[6]Centro de Investigación del Cáncer-Cancer Research Center CSIC-University of Salamanca, Campus Unamuno, 37007 Salamanca Spain

Summary

The immunological synapse (IS) serves a dual role for sustained T cell receptor (TCR) signaling and for TCR downregulation. TC21 (*Rras2*) is a RRas subfamily GTPase that constitutively associates with the TCR and is implicated in tonic TCR signaling by activating phosphatidylinositol 3-kinase. In this study, we demonstrate that TC21 both co-translocates with the TCR to the IS and is necessary for TCR internalization from the IS through a mechanism dependent on RhoG, a small GTPase previously been associated with phagocytosis. Indeed, we found that the TCR triggers T cells to phagocytose 1-6 μm beads through a TC21- and RhoG-dependent pathway. We further show that TC21 and RhoG are necessary for the TCR-promoted uptake of major histocompatibility complex (MHC) from antigen presenting cells. Therefore, TC21- and RhoG-dependence underlie the existence of a common phagocytic mechanism that drives TCR internalization from the IS together with its peptide-MHC ligand.

[7]To whom correspondence should be addressed at balarcon@cbm.uam.es.

Introduction

The immunological synapse (IS) was first described as a highly specialized junction between the membranes of T cells and antigen-presenting cells (APCs; reviewed in (Fooksman et al. 2010). It is characterized by the formation of a central supramolecular activation cluster (cSMAC), where the T cell antigen receptor (TCR) and intracellular signaling molecules such as the Lck and PKCθ kinases are enriched. The cSMAC is surrounded by an integrin-rich peripheral supramolecular activation cluster (pSMAC) (Monks et al., 1998). The IS was proposed to be a site for effective T cell activation, for sustained TCR engagement and signaling, and for polarized secretion into the synaptic space (reviewed in (Balagopalan et al., 2009; Fooksman et al. 2010). However, several studies have shown that T cell activation can be induced prior to, or even in the absence of cSMAC formation, leaving the role of the IS controversial and unclear (Lee et al., 2002; reviewed in Seminario and Bunnell, 2008; Yokosuka and Saito, 2010). It has been proposed that the IS serves to boost TCR triggering when T cells are exposed to low concentrations of peptide antigen-major histocompatibility complex (pMHC) ligand, while promoting TCR downregulation at high pMHC concentrations (Cemerski et al., 2008). Thus, the cSMAC has been proposed as a site of TCR endocytosis and signal extinction.

In resting T cells, the TCR is continuously being endocytosed and re-expressed at the cell surface [reviewed in (Alcover and Alarcon, 2000)]. However, when engaged by pMHC, the TCR is downregulated from the cell surface as a result of increased TCR internalization, decreased recycling and increased degradation. Clathrin-dependent endocytosis is one of the mechanisms by which the TCR is internalized, both in untriggered and TCR triggered cells (Dietrich et al., 1994; Monjas et al., 2004). However, the TCR is also internalized by clathrin-independent mechanisms that share a common cholesterol dependency but are not yet molecularly characterized (Monjas et al., 2004).

Another consequence of IS formation is the intercellular transfer of APC membrane proteins to the T cell. T cells acquire MHC class I and class II glycoproteins from APCs, together with co-stimulatory molecules and membrane patches, by a mechanism referred to as trogocytosis (Ahmed et al., 2008; Davis, 2007; Joly and Hudrisier, 2003; Wetzel and Parker, 2006). MHC transfer to the T cell is TCR triggering-dependent, and it is potentiated by the T cell co-stimulatory molecule CD28 and by CD2 (Hwang et al., 2000; Singleton et al., 2006). The transfer of pMHC to T cells has been demonstrated both *in vitro* and *in vivo* (Huang et al., 1999), although the mechanisms, and physiological meaning of such transfer are not completely understood.

TC21 (*Rras2*) is a small GTPase of the RRas subfamily with strong transformation activity *in vitro* (Graham et al., 1994), which has been implicated in different types of human carcinomas (Arora et al., 2005; Clark et al., 1996; Chan et al., 1994; Sharma et al., 2005). TC21 activates phosphatidylinositol 3-kinase (PI3K) probably through the direct binding and recruitment of the hematopoietic-specific catalytic subunit p110δ (Delgado et al., 2009; Murphy et al., 2002; Rodriguez-Viciana et al., 2004; Rosario et al., 2001). Thus, TC21 has been proposed to activate survival pathways that depend on PI3K activity and that of its effector, Akt (Delgado et al., 2009; Rong et al., 2002). Indeed, *Rras2*$^{-/-}$ mice present normal

lymphoid development but reduced number of mature T and B lymphocytes (Delgado et al., 2009). This reduction in T and B cell number is due to poorer survival and homeostatic proliferation, reflecting the defective activation of tonic housekeeping PI3K. Indeed, TC21 binds directly to the TCR and BCR (B cell antigen receptor) and it is necessary for the recruitment of p110δ to both antigen receptors in resting cells. TC21 is constitutively associated to the TCR and BCR and it has been shown to co-translocate with the TCR to the IS (Delgado et al., 2009).

In this study, we have further investigated the role of TC21 in the formation of the IS. We found that TC21 is necessary for TCR internalization from the IS by a clathrin-independent mechanism but dependent on the small GTPase RhoG, previously associated with phagocytosis. Indeed, we found that T cells phagocytose 1-6 μm beads coated with anti-TCR antibodies through a TC21 and RhoG-dependent pathway. Since TC21-deficient and RhoG-deficient T cells are unable to trogocytose MHC class II and membrane fragments from the APC, we propose that the TCR is internalized from the IS by phagocytosis.

Results

TC21- and RhoG-dependent internalization of the TCR from the immunological synapse

We previously found that TC21 is co-translocated with the TCR to the IS where they both accumulate at the cSMAC (Delgado et al., 2009). To study the behavior of both proteins in the IS, we used time-lapse confocal videomicroscopy of human Jurkat T cells co-transfected with fluorescent-tagged fusion proteins and stimulated with Raji APCs loaded with staphylococcal enterotoxin E (SEE) ‘superantigen’. TC21 and the TCR became first concentrated at the IS within 2 min of the initial contact with an APC (labeled a in Fig. 1A) and later (3-6 min) in a region of the cytoplasm underlying the IS. After 7 min, both proteins had clearly been internalized from the IS and co-localized in internal vesicles, while the T cell began to form another IS with a second APC (labeled b in Fig. 1A and Supplementary Movie 1). After 15-20 min, it was possible to see how part of the internalized TCR translocated from intracellular vesicles to the second IS (Fig. 1A and Supplementary Movie 1). The intensity correlation analysis (ICA) showed a high degree of co-localization between TC21 and the TCR in IS-derived internal vesicles (Supplementary Fig. S1A). After visualizing 10 time-lapse movies, we calculated that 88% of the IS-derived TCR positive vesicles (n= 24) were positive for TC21 (data not shown). These results indicated that TC21 and the TCR follow a common internalization pathway from the IS.

To demonstrate if TC21 influences TCR internalization, Jurkat cells were co-transfected with a fluorescence-tagged subunit of the TCR, and either an inactive (S28N) or a permanently active (G23V) mutant of TC21. The S28N mutant was co-translocated with the TCR to the IS but their internalization was blocked (time 19 min, Fig 1B and Supplementary Fig. S1B). Likewise, expression of G23V TC21 almost completely blocked TCR internalization from the IS; only a small amount of the TCR was internalized in TC21-negative vesicles (arrowhead, Fig. 1B, and Supplementary Fig. S1C). Quantification of the effect of both TC21 mutants on TCR internalization from the IS is shown in Fig. 1C. Interestingly, G23V TC21 expression caused the generation of extensive lamellipodia and large membrane protrusions (bright field, time 25 min, Fig. 1B), suggesting that active TC21

promotes actin cytoskeleton remodeling. In addition, the inhibitory effect of the active G23V TC21 mutant suggests that for TCR internalization TC21 must be able to cycle between the active and the inactive states.

The TCR is endocytosed by both clathrin-dependent and clathrin-independent mechanisms (Dietrich et al., 1994; Monjas et al., 2004). The TCR and TC21 co-localized in internal vesicles derived from the IS that did not contain transferrin or the clathrin heavy chain (Fig. 2A and Supplementary Fig. S2A and S2B). These data suggest TC21 mediated TCR internalization from the IS by clathrin-independent mechanisms. To further study this process, we allowed T cells to adhere to surfaces patterned with focal spots of anti-CD3 surrounded by the integrin ligand ICAM-1. T cells form a structure reminiscent of an IS, with a cSMAC and a pSMAC (Doh and Irvine, 2006). The T cell body was unroofed and prepared for electron microscopy to show the organization of the cytoplasmic side of the plasma membrane. The cytoskeleton was extensively polymerized in the pSMAC area, while the cSMAC was practically devoid of any structure (Fig. 2B, micrograph a). Furthermore, after more vigorous sonication to remove the actin ring, clathrin-coated pits were found abundant in the pSMAC (arrows, Fig. 2B, micrograph c), but they were not detected in the cSMAC (micrograph b; quantification in d). Finally, to prove the clathrin-independence of TCR and TC21 co-internalization, a combination of siRNAs for clathrin heavy chain was transfected to reduce the expression of this protein by 96% (Supplementary Fig. S2C). Clathrin depletion abrogated the endocytosis of transferrin (Fig. S2D) and partly inhibited TCR downregulation (Fig. S2E), but did not affect the co-internalization of the TCR with TC21 from the IS (Fig. S2F and S2G). These results further support the idea of a clathrin-independent mechanism for TCR internalization from the cSMAC.

To characterize the TC21-dependent TCR endocytotic process, we co-transfected Jurkat cells with different combinations of CD3ζ, TC21 and other GTPases known to be associated with early endosomes (Rab4 and Rab5), fast (Rab4) and slow (Rab11) recycling endosomes, late endosomes (Rab7) and phagosomes (Rab5 and Rab7; Supplementary Fig. S3A) (Zerial and McBride, 2001). Vesicles containing TC21 only partially coincided with these Rab GTPases. However the co-localization of TCR internalized from the IS with the RhoG GTPase was extensive (Fig. 2C, Supplementary Movie 2 and Supplementary Fig. S1D) as illustrated by the redistribution of RhoG from a homogenously cytoplasmic to a concentrated localization in the CD3ζ-positive IS-derived vesicles (compare time points 0 and 2 min in Fig. 2C). Indeed 100% of the TCR vesicles derived from the IS (n=15 vesicles from 11 movies) were positive for RhoG (data not shown). The internalization of the TCR from the IS into RhoG-positive vesicles suggests that RhoG might be involved in TCR internalization from the IS.

RhoG is an important, evolutionarily conserved, intracellular mediator of the phagocytosis of apoptotic cells (deBakker et al., 2004; Henson, 2005), which lies upstream of the Rac1 GTPase, a regulator of actin polymerization (Groves et al., 2008; Niedergang and Chavrier, 2005). In addition, RhoG is involved in caveolar endocytosis (Prieto-Sanchez et al., 2006). T cells do not have caveolin, yet the TCR can be internalized in a manner that is cholesterol-dependent and clathrin-independent (Monjas et al., 2004). The expression of either inactive (T17N) or constitutively active (Q61L) mutants of RhoG. inhibited the internalization of the

TCR (Fig. 2D and 2F) and of TC21 (Fig. 2E and 2F, and Supplementary Movie 3) from the IS by 80-90%. These results indicate that TCR and TC21 internalization from the IS requires RhoG activity.

T cells phagocytose by a TCR-triggered TC21 and RhoG-dependent process

Time-lapse confocal videomicroscopy (Fig. 1A and Supplementary Movie 1) showed that T cells embrace and try to engulf the APC. This is reminiscent of incomplete phagocytosis. In addition, RhoG has been functionally linked to phagocytosis in different systems and organisms (Henson, 2005). If T cells were not able to complete phagocytosis due to the size of the APC, we considered it interesting to test whether T cells could phagocytose smaller surrogate APCs. To this end, we stimulated Jurkat T cells with latex beads of different sizes coated with anti-CD3, a stimulus that has frequently been used to study the formation of structures reminiscent of ISs (Batista et al., 2004; Glebov and Nichols, 2004). Our results showed that Jurkat T cells phagocytosed anti-CD3 coated latex beads of 1, 3 and even 6 μm diameter (Fig. 3A). The phenomenon was not restricted to T cell lines since primary mouse and human T cells were also able to phagocytose anti-CD3-coated beads (Fig. 3A-C). In addition, phagocytosis of latex beads was TCR-dependent since anti-CD3-coated beads were not phagocytosed by a Jurkat mutant that did not express the TCR in the plasma membrane (Supplementary Fig. S3B). Interestingly, mouse naïve T cells could phagocytose anti-CD3-coated 6 μm beads, which are as big as the phagocytic lymphocyte (Fig. 3A and B). This is made possible through an intense redistribution of the T cell plasma membrane, displacing the cytoplasm and nucleus to one pole (Fig. 3A and B).

The T cell plasma membrane forms a tight contact, a process characteristic of phagocytosis (Swanson, 2008), with the antibody-coated bead since a secondary anti-Ig is unable to enter into the gaps formed between T cells and beads (arrowheads, 6 μm beads, Fig. 3A and 3B).. The phagocytosed beads appeared to be surrounded by both the TCR and polymerized actin (Fig. 3C), suggesting that, like other phagocytic processes (Swanson, 2008), TCR-triggered phagocytosis is linked to the rearrangement of the actin cytoskeleton. To prove the dependence of TCR-triggered phagocytosis on actin polymerization, we first set up a quantitative phagocytosis assay based on distinguishing adhered beads from phagocytosed beads according to their accessibility to a secondary anti-Ig fluorescent antibody. With time, there was a clear transfer of cells from the population labeled in green and red (i.e. that had adhered beads) to the population that exclusively had beads inside and only fluoresced red (Fig. 3D). Using this approach, we measured the efficiency of phagocytosis in the presence of the actin cytoskeleton inhibitor cytochalasin D. This inhibitor almost completely abrogated the uptake of anti-CD3-coated beads, independent of their size (Fig. 3E). The requirement for PI3K activity during phagocytosis has also been described in “professional” phagocytes (Yeung and Grinstein, 2007). TCR-triggered phagocytosis of latex beads was also PI3K-dependent as shown by its sensitivity to the class I PI3K inhibitors wortmannin and LY294002 (Fig. 3F). Interestingly, the sensitivity to PI3K inhibition increased as did the size of the phagocytosed particle, in agreement with previous findings for Fc receptors (reviewed in (Yeung and Grinstein, 2007).

The confocal microscopy and flow cytometry experiments clearly indicated that the phagocytosed beads were internal and not exposed to the extracellular milieu. Using electron microscopy we additionally demonstrated that the anti-CD3-coated beads were included in a vesicular compartment and they were not free in the cytoplasm (Fig. 3G). Phagocytic caps around the anti-CD3-coated beads were detected at early time points (5 min, Fig. 3G, micrograph a), whereas later, the phagocytosed beads were found internal and surrounded by a membrane (15 min, Fig. 3G, micrograph b). After longer incubations (30 min, micrograph c), beads were detected in what appear to be multivesicular bodies (MVB), with several beads and vesicles surrounded by an external membrane. Later (1 hr) it was possible to detect beads in the outer part of the plasma membrane, coated with membrane fragments, suggesting that they were first phagocytosed and later secreted (Fig. 3G, micrograph d).

In transfected Jurkat cells, the phagocytosed beads were found in compartments where TC21-green fluoresncent protein (GFP) and RhoG-GFP were present (Fig. 4A). The use of antibodies against the endogenous CD3ζ (Fig. 4A), TC21 and RhoG (Fig. 4B) proteins demonstrated that co-localization of these proteins with phagocytosed beads was not caused by overexpression. Transfection of the dominant negative and constitutively active mutants of both TC21 and RhoG inhibited the phagocytosis of anti-CD3-coated beads (Fig. 4C). This inhibition was dose-dependent, such that cells expressing more of the dominant negative mutants phagocytosed fewer beads (Fig. 4D). These data indicate that overexpression of TC21 and RhoG mutants in a T cell line inhibit TCR-triggered phagocytosis. To confirm these results in a more physiological setting, we studied whether TCR-dependent phagocytosis of latex beads was affected in mice genetically deficient in either TC21 (*Rras2*$^{-/-}$) or RhoG (*Rhog*$^{-/-}$). When analyzed by confocal microscopy and flow cytometry, the phagocytosis of anti-CD3-coated beads was blocked in the absence of either GTPase (Fig. 4E), reinforcing the idea of a complete dependence of TCR-mediated phagocytosis on TC21 and RhoG activities.

TCR downregulation is impaired in genetically deficient T cells

Overexpression of constitutively active and inactive mutants in a T cell line indicated that TC21 and RhoG both mediate the internalization of the TCR from the IS (Fig. 1B-C and 2E-G). To study the role of TC21 and RhoG in TCR internalization from the IS in primary cells, we used T cells from *Rras2*$^{-/-}$ and *Rhog*$^{-/-}$ mice transgenic for TCRs of defined antigen specificity and transduced with CD3ζ-GFP. We used as a model the AND TCR which recognizes the class II MHC allele I-E^{k} bound to an antigenic peptide derived from moth cytochrome c (MCC) and DCEK cells as APCs. Time-lapse confocal videomicroscopy of live WT AND T cells indicated that the TCR rapidly accumulated at the IS (0.48 min Fig. 5A and Supplementary Movie 4) becoming internalized thereafter (0.48-5.30 min, Fig. 5A). However, in AND T cells from *Rras2*$^{-/-}$ and *Rhog*$^{-/-}$mice, the pool of TCR accumulating at the IS was not internalized, even 19 min after stimulation (Fig. 5A and Supplementary Movies 5 and 6). The TCR is internalized both from the IS and from plasma membrane regions distal to the IS (Das et al., 2004). In addition, intracellular TCR-positive vesicles could be part of exocytotic pathways. Therefore, to track TCR^{+} vesicles originated at the IS and distinguish them from vesicles of other origins, the surface of AND T cells was labeled with a poorly stimulatory anti-TCRβ (H57 antibody) before stimulation with MCC-loaded

DCEK cells. Cells with $H57^{+}$ vesicles placed just below the IS were counted as positive for IS-derived TCR internalization. In these experiments, intracellular anti-CD3ζ staining served to track the IS. Accordingly, WT AND T cells (arrowhead, Fig. 5B) but not *Rras2*$^{-/-}$ and *Rhog*$^{-/-}$ T cells were able to internalize the TCR from the IS. Therefore, TC21 and RhoG appear to be necessary for the internalization of the TCR from the IS. The cSMAC is thought to be a site of TCR internalization (Lee et al., 2003). Since TC21 and RhoG deficiency inhibited TCR internalization from the IS by 50-80% (Fig. 1C, 2G and 5B), we considered using TC21- and RhoG-deficient mice to test the importance of TCR internalization from the IS for global TCR downregulation. TCR downregulation was only slightly affected in the absence of either GTPase (20% inhibition, Fig. 5C), suggesting that the bulk of TCR internalization leading to downregulation occurs from sites other than the IS. Interestingly, the inhibition of TCR downregulation in TC21- and RhoG-deficient mice was most pronounced when high concentrations of antigen were used, suggesting that the implication of the IS in TCR downregulation increases with the dose of antigen. Likewise, a mild effect of TC21 and RhoG deficiency on TCR downregulation was only evident after long incubations (Fig. 5D).

Inhibiting TCR downregulation by altering the endocytotic and receptor degradation machineries usually results in a stronger response to antigen, indicating that TCR downregulation primarily produces desensitization (Andre et al., 1997; Dragone et al., 2009; Vardhana et al.). The AND T cells deficient in either TC21 or RhoG showed a stronger response to antigen, measured by CD69 expression and IL-2 release, than the WT controls (Supplementary Fig. S4A and S4B). In addition, we detected a stronger tyrosine phosphorylation of CD3ζ and ERK in TC21-deficient and RhoG-deficient than in WT T cells and also a stronger phosphorylation of Tyr 319 in ZAP70 in TC21-deficient mice (Supplementary Fig. S4D and S4E) suggesting that TCR proximal signaling is also enhanced in the absence of these GTPases. However, both TC21 and RhoG deficiency inhibited the proliferative response to antigen (Supplementary Fig. S4C). These results probably reflect the variety of cellular processes affected by these GTPases. The increased CD69 and IL-2 response in deficient T cells could be secondary to the deficient TCR internalization from the IS Likewise, stimulation of RhoG-deficient T cells with beads of different sizes resulted in a stronger induction of CD69 and stronger proliferation than WT controls (Supplementary Fig. S4F and S4G). Interestingly, TC21-deficient T cells were not more responsive than WT controls (Supplementary Fig. S4F and S4G), indicating that RhoG is more purely involved in TCR-triggered phagocytosis than TC21. In other words, TC21 may regulate additional TCR-triggered processes, such as we have previously shown for TCR tonic signaling (Delgado et al., 2009).

We have previously shown that TCR triggering with soluble anti-CD3 antibody is mediated by clathrin-dependent endocytosis, whereas triggering with anti-CD3 immobilized onto a plastic surface is clathrin-independent (Monjas et al., 2004). These two processes were differentially affected by TC21 and RhoG deficiencies. Thus, TCR downregulation after stimulation with immobilized anti-CD3 was significantly inhibited in the absence of these GTPases, whereas TCR downregulation after stimulation with soluble anti-CD3 was not (Supplementary Fig. S5A). These results set a parallelism between TCR downregulation

from the IS (Fig. 5C and 5D) and TCR downregulation provoked by immobilized anti-CD3. Consequent with the desensitization role of TCR downregulation mediated by TC21 and RhoG, T cell proliferation in response to immobilized anti-CD3, was enhanced in the absence of TC21 and RhoG but was not affected if soluble anti-CD3 was used as a stimulus (Supplementary Fig. S5B).

TC21 and RhoG mediate TCR-triggered trogocytosis of MHC

Despite the clear capacity of the TCR to trigger the phagocytosis of large particles by T cells, T cells are not meant to phagocytose latex beads. Thus, we wondered whether TCR-driven phagocytosis of beads reflected the participation of TC21 and RhoG in the processes of trogocytosis and TCR internalization from the IS. In other words, the phagocytosis of beads and TCR internalization may recreate a trogocytotic process when the T cell is stimulated by an antigen-loaded APC. To determine how TC21 and RhoG deficiencies affect TCR-mediated trogocytosis, AND WT and mutant T cells were stimulated with MCC-loaded DCEK cells previously labeled with the lypophilic PKH26 red fluorescent dye. Upon stimulation, WT AND T cells acquired fragments of the DCEK membrane that were detected by flow cytometry and by confocal microscopy as 0.5 μm-1μm red vesicles inside T cells (Fig. 6A). The acquisition of APC membrane fragments by WT T cells was also observed in $CD8^+$ T cells bearing the OT-I TCR transgene (Supplementary Movie 7). However, *Rras2*$^{-/-}$ and *Rhog*$^{-/-}$ AND and OT-I T cells had reduced capacity to take APC membrane fragments labeled with PKH26 (Fig. 6A, and data not shown). The TC21 and RhoG dependence of TCR-driven trogocytosis of APC membrane fragments parallels their role in TCR-driven phagocytosis of latex beads. Indeed, TCR-triggered trogocytosis was inhibited by wortmannin and LY294002 (Fig. 6B), indicating that like phagocytosis (Fig. 3F), trogocytosis is mediated by PI3K activation. Together, these results indicate that the accumulation of the TCR at the IS results in the TCR-triggered acquisition of APC membrane fragments accompanied by the internalization of the TCR from the IS. Indeed, both these processes are mediated by a PI3K-dependent phagocytotic mechanism in which TC21 and RhoG play an important role.

TCR-dependent trogocytosis of APC membrane fragments by T cells is accompanied by the acquisition of MHC (Hwang et al., 2000). To study the TCR-driven acquisition of MHC by T cells, we used MCC-loaded DCEK cells transiently transfected with an I-$E^K\alpha$-GFP fusion protein. Using time-lapse confocal videomicroscopy we observed that naïve WT AND T cells (Fig. 6C and Supplementary Movie 8), but not TC21- or RhoG-deficient T cells (data not shown), acquired I-$E^K\alpha$-GFP from the APC at the T cell:APC contact site, indicating that membrane fragments containing I-$E^K\alpha$-GFP were acquired from the IS and not by phagocytosis of exosomes. In fixed cells, we found that the I-$E^K\alpha$-GFP protein was acquired by WT T cells, but not by TC21- or RhoG-deficient cells, and was associated to internalized TCR in 0.5 μm-1μm vesicles (Fig. 6D). Flow cytometry data indicated that the uptake of I-$E^K\alpha$-GFP by WT AND T cells was dependent on the dose of antigen (Fig. 6D). These data support the idea that T cells try to phagocytose the APC but instead take fragments of the APC membrane at the IS by a phagocytic mechanism mediated by TC21 and RhoG.

TCR triggering activates RhoG by a TC21 and PI3K-dependent mechanism

We next used TC21- and RhoG-deficient T cells to elucidate their relative position in the TCR signaling pathway. It is not known if the TCR can regulate RhoG activity. We stimulated Jurkat cells with anti-CD3 coated latex beads and measured the amount of active (GTP-bound) RhoG recovered from the cells with a glutathione-S-transferase (GST) fusion protein of the Ras-binding domain (RBD) of engulfment and motility protein (ELMO), an effector of RhoG. TCR triggering promoted the activation of RhoG (Fig. 7A). Likewise, stimulation of AND WT T cells with the MCC antigen activated RhoG as well (Fig. 7B). RhoG activation was weaker in TC21-deficient cells than in WT T cells (Fig. 7B), suggesting that TC21 lies upstream of RhoG in the TCR signal transduction cascade. In other phagocytic systems, RhoG is situated downstream of PI3K since the RhoG activator TRIO is PI3K-dependent (Henson, 2005), while in T cells TC21 is a direct effector of the TCR in the PI3K pathway (Delgado et al., 2009). Thus, we analyzed whether PI3K activation was affected by TC21 deficiency in conditions of phagocytosis and trogocytosis. We found that in the absence of TC21, Akt phosphorylation was slower, weaker and less sustained than in WT T cells stimulated with antigen (Fig. 7C) or anti-CD3 coated beads (Fig. 7D). Furthermore, RhoG activation but not TC21 activation by the TCR was sensitive to inhibition of PI3K activity (Fig. 7E). The effects of TC21-deficiency on RhoG and Akt activities induced by TCR triggering were not complete (Fig. 7B, 7C and 7D), suggesting that alternative routes play a partly redundant role. If RRas or classical Ras family members are responsible for the TC21-independent activities warrants further investigation.

These results were consistent with the hypothesis that TC21 mediates the activation of RhoG by the TCR in conditions leading to phagocytosis. Therefore, the orderly participation of these elements would be such that the TCR accumulates at the cSMAC, activates TC21 and TC21 promotes the activation of RhoG via PI3K.

Discussion

In this study we have provided evidence that phagocytosis underlies several key aspects of T cell biology and that the Ras family GTPases TC21 and RhoG mediate this process. We have shown that T cells can phagocytose large inert particles (1-6 μm) coated with an antibody that triggers the TCR through a process that requires TC21 and RhoG. Indeed, the internalization of the TCR from the IS is inhibited in the absence of TC21 or RhoG, as is the uptake of APC membrane fragments and the MHC complex by the T cell. Together, our data favor a model in which T cells embrace and try to engulf antigen loaded APCs, resulting in the polymerization of the actin cytoskeleton and the spread of the T cell membrane over the APC surface.

The spread of the T cell membrane is driven by an actin ring (Barda-Saad et al., 2005) similar to the ring formed around particles at the tip of the phagocytic cups formed by “professional” phagocytes, and when adhered to planar surfaces (Gerisch et al., 2009). The initial expansion of the actin ring is followed by a contraction that could parallel the closing of the phagocytic cup (Supplementary Fig. S6). This contraction is accompanied by a centripetal movement of the TCRs to the center of the IS, resulting in their accumulation in the cSMAC (Yokosuka and Saito). Finally, the TCR is internalized from the cSMAC by a

process that requires the activity of TC21 and RhoG. The TCR is internalized from the cSMAC in association with fragments of the APC. The resulting process is a frustrated phagocytosis of the whole APC by the T cell that instead trogocytoses APC fragments (Supplementary Fig. S6). Interestingly, Wülfing and colleagues, nicely showed by electron microscopy how a large invagination in the T cell is formed around a fragment of the APC in a TCR affinity-dependent manner (Singleton et al., 2006). The molecular mechanisms that allow the phagocytic cup to close around the APC membrane fragment are at present unknown.

The result of this process is the removal of an APC fragment and the internalization of the TCR from the cSMAC. However, it remains unclear what is the destiny of the internalized TCR and its accompanying APC membrane fragment. Our electron microscopy data on phagocytosed anti-CD3-coated beads indicate that the phagoytosed material localizes in MVBs (Saksena et al., 2007). This is consistent with the described role of the ESCRT-I component TSG101 in cSMAC formation and TCR downregulation (Vardhana et al.). From these MVBs, the TCR and trogocytosed APC membrane fragments can be either destined for degradation or recycled to the T cell's plasma membrane. Indeed, some of our data indicate that the internalized TCR and its accompanying APC fragments are recycled to the plasma membrane. In this way, the T cell could express the pMHC complex acquired from the APC and become an APC itself. We do not yet know the physiological meaning of this conversion, which remains controversial. It is unclear whether the acquisition of MHC by the T cell is a mechanism to remove pMHC and negatively control the immune response, or whether it is a mechanism to potentiate the immune response by converting the T cell into an efficient APC (Smyth et al., 2007; Umeshappa et al., 2009). The TC21- and RhoG-deficient mice could become an important tool to study the relevance of T cells converted into APCs in the immune response.

The signaling subunits of the TCR bear tyrosine and leucine containing signaling motifs known as immunoreceptor based tyrosine activation motifs (ITAMs), which are phosphorylated by tyrosine kinases of the src family converting them into docking sites for tyrosine kinases of the Syk family. Fc**γ**Rs also bear ITAMs that mediate Fc**γ**R triggered phagocytosis (Cox and Greenberg, 2001). Therefore, it should not be surprising if the TCR also triggers phagocytosis through its ITAMs. The participation of TC21 in TCR signaling does not seem to follow the canonical pathway, involving tyrosine phosphorylation of the ITAMs, Src and Syk kinases, since TC21 directly binds non-phosphorylated ITAMs (Delgado et al., 2009). Hence, it is appealing to hypothesize that TC21 may also participate in Fc**γ**R-triggered phagocytosis via its ITAMs.

In resting T cells the TCR is internalized and recycled to the plasma membrane. However, TCR triggering results in the downregulation of the TCR from the cell surface by mechanisms that involve increased internalization, decreased recycling and increased degradation (Alcover and Alarcon, 2000). The TCR seems to be internalized by a clathrin-dependent pathway and at least one other clathrin-independent pathway (Monjas et al., 2004). By using T cells that express two TCRs of different specificity for pMHC, and T cells that express a full TCR and a chimera bearing cytoplasmic tails of the TCR signaling subunits, TCR triggering has been shown to provoke the downregulation of the engaged and

the non-engaged TCRs (Fernandez-Miguel et al., 1999; Monjas et al., 2004; Niedergang et al., 1997; San Jose et al., 2000; von Essen et al., 2006). Furthermore, through pharmacological and dominant negative approaches, we showed that non-engaged TCRs are downregulated by a clathrin-dependent mechanism while the engaged TCRs are primarily downregulated by a mechanism independent of clathrin (Monjas et al., 2004). The results shown in the present study further support this notion since they provide evidence that the engaged TCRs present in the cSMAC are downregulated by a phagocytic mechanism mediated by TC21 and RhoG. Indeed, one of our previous findings indicated that clathrin-dependent endocytosis predominates as a mechanism for TCR internalization when low doses of antigen or anti-CD3 stimulus are used, while the clathrin-independent mechanism becomes more important at high doses of ligand and, therefore, more TCR engagement (Monjas et al., 2004; San Jose et al., 2000). The results shown here also indicate that TCR downregulation is only inhibited, although partially, in the absence of TC21 and RhoG in the presence of high doses of antigen. Although a possible redundancy of TC21 and RhoG with RRas and classical Ras or Rho subfamily GTPases cannot be at present excluded, our results suggest that clathrin-mediated TCR internalization is predominant and that internalization of the engaged TCRs from the cSMAC by phagocytosis is less important and only significant for overall TCR downregulation at high antigen concentrations. Indeed, we show in this paper that reduced expression of clathrin heavy chain had an important impact on TCR downregulation although, as expected, the inhibition was not complete. It remains to be determined if abrogation of both the TC21 and RhoG phagocytic pathway and the clathrin endocytosis pathway result in a complete blockade of TCR downregulation.

This study also sheds light on the role of TCR downregulation. TC21 and RhoG deficient T cells show enhanced response to antigen stimulation, suggesting that one of the consequences of TCR downregulation is the termination of TCR signaling. This is in agreement with the effect on T cell activation of disabling other proteins involved in TCR internalization and endocytosis (Andre et al., 1997; Dragone et al., 2009; Vardhana et al.). In the absence of TC21 or RhoG, the TCR remains at the IS and it signals for longer, similar to the effects of TSG101 depletion (Vardhana et al.), suggesting that if the TCR is not internalized from the IS the TCR signal is sustained. This is consistent with the idea that TCR downregulation is a consequence of TCR signaling and that it serves to terminate TCR signaling. This explains why stronger ligands promote TCR downregulation from the IS faster than weaker ligands (Cemerski et al., 2008).

In conclusion, we have shown that the TCR is internalized from the IS by phagocytosis, which requires the participation of the Ras family GTPases TC21 and RhoG. This phagocytotic internalization of the TCR is accompanied by the uptake of APC membrane fragments that include MHC complexes. Further studies will be necessary to determine precisely how TC21 and RhoG are integrated into the TCR phagocytic signaling pathway, the implication of TC21 in the phagocytosis promoted by other receptor types, and the relevance of the phagocytic uptake of pMHC complexes by T cells in the overall T cell response to antigen.

Experimental Procedures

Cells and mice

The human Jurkat T cell lymphoma and the human lymphoblastoid B cell line Raji were grown in RPMI plus 5% fetal bovine serum (FBS). The DCEK fibroblast cell line stably transfected with plasmids encoding I-E^k and CD80, and Human Embryonic Kidney (HEK) 293T cells, were grown in DMEM plus 10% FBS. Lymph node T cells were maintained in RPMI 10% FBS supplemented with 20 μM β-mercaptoethanol and 10 mM sodium pyruvate. *Rras2*$^{-/-}$ and *Rhog*$^{-/-}$ mice were generated as described previously (Delgado et al., 2009; Vigorito et al., 2004). *Rras2*$^{-/-}$ and *Rhog*$^{-/-}$mice were crossed with mice transgenic for the OT-I TCR (OVAp specific. H-2K^b restricted) (Hogquist et al., 1994) and for the AND TCR (MCC specific, I-E^k restricted) (Kaye et al., 1989), and the resulting heterozygous mice were crossed again to generate TCR transgenic wild type and genetically targeted homozygous mice. All experiments involved the use of littermates homozygous for the wild type or the knockout alleles. Mice were maintained under SPF conditions in the animal facility of the 'Centro de Biología Molecular Severo Ochoa' in accordance with applicable national and European guidelines. All animal procedures were approved by the ethical committee of the 'Centro de Biología Molecular Severo Ochoa'.

Time-lapse fluorescence confocal microscopy and immunofluorescence

Jurkat cells and preactivated transduced T cells from WT, *Rras2*$^{-/-}$ or *Rhog*$^{-/-}$ mice were adhered to fibronectin-coated plates in 1ml of HBSS containing either 2% or 10% of FBS (for Jurkat and primary cells, respectively), and they were placed on a microscope stage and maintained at 37°C. Antigen presenting cells (Raji, DCEKs, or T2-K^b cells) preloaded with antigen (SEE, MCC or OVAp) were added, and a series of fluorescence and brightfield frames were captured sequentially every 5, 30 or 60 seconds, depending on the experiment. Two confocal microscope systems were used: a Zeiss LSM510 META coupled to an Axiovert200 inverted microscope; and a LSM710 coupled to an AxioObserver inverted microscope with 63x and 100x PlanApo oil immersion objectives (1.4 numerical aperture). The images were processed and videos were generated using Metamorph software 6.2r6 (Universal Imaging).

For confocal microscopy, cells were first adhered to poly-L-lysine-coated coverslips, and they were then fixed and permeabilized as described previously (Delgado et al., 2009), prior to staining with the appropriate antibodies. An inverted Axiovert200M microscopy system coupled to a Confocal LSM510 was used with 63x PlanApo oil immersion objective lens (1.4 numerical aperture) and 100x Plan-Neofluar oil immersion objective lens (1.3 numerical aperture). For immunofluorescence of cells phagocytosing latex beads, spectral imaging and linear unmixing was used to separate different emissions. For quantification of TCR and TC21 internalization from the IS, T cell:APC conjugates were photographed with the 100x Plan-Neofluar objective at a resolution of 1024×1024 pixels and the presence of intracellular vesicles derived from the IS was evaluated according to their distance to the IS (<1.4 μm) and the existence of a gap between the vesicle and the IS ≥300 nm. For co-localization analysis, 12 bit images were subjected to background correction and threshold-based analysis using Image J software. Quantitative co-localization was carried out using the

Intensity Correlation Analysis (ICA) imaging method as described (Li et al., 2004). These methods are briefly explained in Supplemental Experimental Procedures.

Phagocytosis and trogocytosis assays

Jurkat or naïve cells were resuspended in RPMI containing 20mM HEPES [pH 7.4] plus 0.2% BSA, and pre-incubated for 1hr at 37°C. Inhibitors were added during the last 30 min of the preincubation and the cells were then plated in 96-well V-bottom plates at a density of 2×10^5 (Jurkat) or 5×10^5 (primary) cells in 25 μl of medium. Antibody-coated beads (prepared as indicated in Supplemental Experimental Procedures) were added in 25 μl of medium to reach a cell:bead ratio of 1:50 (Jurkat) or 1:10 (primary cells). The cell:bead suspension was briefly centrifuged at 900 g to bring the cells and beads into close contact, and they were then incubated at 37°C. Subsequently, the cells were washed and stained with a fluorescent isotype-specific anti-Ig antibody to track the presence of beads bound to the cells that had not yet been phagocytosed. At this stage, the cells were either analyzed by flow cytometry or incubated for 15 min on coverslips coated with poly-L-lysine, and then processed for immunofluorescence as indicated above.. All the procedures to quantify the internalization of the patches of APC membrane labeled with PKH26, and to follow the uptake of I-E^k, were performed according to the protocol described previously (Daubeuf et al., 2006).

Statistical analysis

Quantitative data are shown as the means ± SD. A non-parametric two-tailed Mann-Whitney test was used to assess the confidence intervals using the Graph Path Prism software.

Antibodies and other reagents

A full list of antibodies and other reagents used are shown as Supplemental Experimental Procedures.

Supplementary Material

Refer to Web version on PubMed Central for supplementary material.

Acknowledgments

We wish to thank Mark Davis, Ed Palmer, Rafa Samaniego and Marino Zerial for kindly providing us with reagents, and Florence Niedergang, Klaus Okkenhaug and Mark Sefton for critical reading of the manuscript. We are also indebted to Cristina Prieto, Valentina Blanco, Tania Gómez and the Confocal Microscopy Unit for their expert technical assistance. This work was supported by grants SAF2006-01391 and SAF2010-14912 from CICYT, SAL-0159/2006 from the Comunidad de Madrid, RD06/0020/1002 and RD06/0020/0001 from RETICS, FP7/2007-2013 from the EU and from ‘Fundación Científica de la Asociación Española Contra el Cáncer’. Institutional support from the Fundación Ramón Areces to the CBMSO is also acknowledged.

References

Ahmed KA, Munegowda MA, Xie Y, Xiang J. Intercellular trogocytosis plays an important role in modulation of immune responses. Cell Mol Immunol. 2008; 5:261–269. [PubMed: 18761813]

Alcover A, Alarcon B. Internalization and intracellular fate of TCR-CD3 complexes. Crit Rev Immunol. 2000; 20:325–346. [PubMed: 11100805]

Andre P, Boretto J, Hueber AO, Regnier-Vigouroux A, Gorvel JP, Ferrier P, Chavrier P. A dominant-negative mutant of the Rab5 GTPase enhances T cell signaling by interfering with TCR down-modulation in transgenic mice. J Immunol. 1997; 159:5253–5263. [PubMed: 9548464]

Arora S, Matta A, Shukla NK, Deo SV, Ralhan R. Identification of differentially expressed genes in oral squamous cell carcinoma. Mol Carcinog. 2005; 42:97–108. [PubMed: 15599930]

Balagopalan L, Barr VA, Samelson LE. Endocytic events in TCR signaling: focus on adapters in microclusters. Immunol Rev. 2009; 232:84–98. [PubMed: 19909358]

Barda-Saad M, Braiman A, Titerence R, Bunnell SC, Barr VA, Samelson LE. Dynamic molecular interactions linking the T cell antigen receptor to the actin cytoskeleton. Nat Immunol. 2005; 6:80–89. Epub 2004 Nov 2021. [PubMed: 15558067]

Batista A, Millan J, Mittelbrunn M, Sanchez-Madrid F, Alonso MA. Recruitment of transferrin receptor to immunological synapse in response to TCR engagement. J Immunol. 2004; 172:6709–6714. [PubMed: 15153487]

Borroto A, Lama J, Niedergang F, Dautry-Varsat A, Alarcon B, Alcover A. The CD3 epsilon subunit of the TCR contains endocytosis signals. J Immunol. 1999; 163:25–31. [PubMed: 10384095]

Cemerski S, Das J, Giurisato E, Markiewicz MA, Allen PM, Chakraborty AK, Shaw AS. The balance between T cell receptor signaling and degradation at the center of the immunological synapse is determined by antigen quality. Immunity. 2008; 29:414–422. Epub 2008 Aug 2028. [PubMed: 18760640]

Clark GJ, Kinch MS, Gilmer TM, Burridge K, Der CJ. Overexpression of the Ras-related TC21/R-Ras2 protein may contribute to the development of human breast cancers. Oncogene. 1996; 12:169–176. [PubMed: 8552388]

Cox D, Greenberg S. Phagocytic signaling strategies: Fc(gamma)receptor-mediated phagocytosis as a model system. Semin Immunol. 2001; 13:339–345. [PubMed: 11708889]

Chan AM, Miki T, Meyers KA, Aaronson SA. A human oncogene of the RAS superfamily unmasked by expression cDNA cloning. Proc Natl Acad Sci U S A. 1994; 19:7558–7562. [PubMed: 8052619]

Das V, Nal B, Dujeancourt A, Thoulouze MI, Galli T, Roux P, Dautry-Varsat A, Alcover A. Activation-induced polarized recycling targets T cell antigen receptors to the immunological synapse; involvement of SNARE complexes. Immunity. 2004; 20:577–588. [PubMed: 15142526]

Daubeuf S, Puaux AL, Joly E, Hudrisier D. A simple trogocytosis-based method to detect, quantify, characterize and purify antigen-specific live lymphocytes by flow cytometry, via their capture of membrane fragments from antigen-presenting cells. Nat Protoc. 2006; 1:2536–2542. [PubMed: 17406507]

Davis DM. Intercellular transfer of cell-surface proteins is common and can affect many stages of an immune response. Nat Rev Immunol. 2007; 7:238–243. Epub 2007 Feb 2009. [PubMed: 17290299]

deBakker CD, Haney LB, Kinchen JM, Grimsley C, Lu M, Klingele D, Hsu PK, Chou BK, Cheng LC, Blangy A, et al. Phagocytosis of apoptotic cells is regulated by a UNC-73/TRIO-MIG-2/RhoG signaling module and armadillo repeats of CED-12/ELMO. Curr Biol. 2004; 14:2208–2216. [PubMed: 15620647]

Delgado P, Cubelos B, Calleja E, Martinez-Martin N, Cipres A, Merida I, Bellas C, Bustelo XR, Alarcon B. Essential function for the GTPase TC21 in homeostatic antigen receptor signaling. Nat Immunol. 2009; 10:880–888. Epub 2009 Jun 2028. [PubMed: 19561613]

Dietrich J, Hou X, Wegener AM, Geisler C. CD3 gamma contains a phosphoserine-dependent di-leucine motif involved in down-regulation of the T cell receptor. Embo J. 1994; 13:2156–2166. [PubMed: 8187769]

Doh J, Irvine DJ. Immunological synapse arrays: patterned protein surfaces that modulate immunological synapse structure formation in T cells. Proc Natl Acad Sci U S A. 2006; 103:5700–5705. Epub 2006 Apr 5703. [PubMed: 16585528]

Dragone LL, Shaw LA, Myers MD, Weiss A. SLAP, a regulator of immunoreceptor ubiquitination, signaling, and trafficking. Immunol Rev. 2009; 232:218–228. [PubMed: 19909366]

Fernandez-Miguel G, Alarcon B, Iglesias A, Bluethmann H, Alvarez-Mon M, Sanz E, de la Hera A. Multivalent structure of an alphabetaT cell receptor. Proc Natl Acad Sci U S A. 1999; 96:1547–1552. [PubMed: 9990061]

Fooksman DR, Vardhana S, Vasiliver-Shamis G, Liese J, Blair DA, Waite J, Sacristan C, Victora GD, Zanin-Zhorov A, Dustin ML. Functional anatomy of T cell activation and synapse formation. Annu. 28:79–105.

Gerisch G, Ecke M, Schroth-Diez B, Gerwig S, Engel U, Maddera L, Clarke M. Self-organizing actin waves as planar phagocytic cup structures. Cell Adh Migr. 2009; 3:373–382. Epub 2009 Oct 2001. [PubMed: 19855162]

Glebov OO, Nichols BJ. Lipid raft proteins have a random distribution during localized activation of the T-cell receptor. Nat Cell Biol. 2004; 6:238–243. Epub 2004 Feb 2008. [PubMed: 14767481]

Graham SM, Cox AD, Drivas G, Rush MG, D'Eustachio P, Der CJ. Aberrant function of the Ras-related protein TC21/R-Ras2 triggers malignant transformation. Mol Cell Biol. 1994; 14:4108–4115. [PubMed: 8196649]

Groves E, Dart AE, Covarelli V, Caron E. Molecular mechanisms of phagocytic uptake in mammalian cells. Cell Mol Life Sci. 2008; 65:1957–1976. [PubMed: 18322649]

Henson PM. Engulfment: ingestion and migration with Rac, Rho and TRIO. Curr Biol. 2005; 15:R29–30. [PubMed: 15649349]

Hogquist KA, Jameson SC, Heath WR, Howard JL, Bevan MJ, Carbone FR. T cell receptor antagonist peptides induce positive selection. Cell. 1994; 76:17–27. [PubMed: 8287475]

Huang JF, Yang Y, Sepulveda H, Shi W, Hwang I, Peterson PA, Jackson MR, Sprent J, Cai Z. TCR-Mediated internalization of peptide-MHC complexes acquired by T cells. Science. 1999; 286:952–954. [PubMed: 10542149]

Hwang I, Huang JF, Kishimoto H, Brunmark A, Peterson PA, Jackson MR, Surh CD, Cai Z, Sprent J. T cells can use either T cell receptor or CD28 receptors to absorb and internalize cell surface molecules derived from antigen-presenting cells. J Exp Med. 2000; 191:1137–1148. [PubMed: 10748232]

Joly E, Hudrisier D. What is trogocytosis and what is its purpose? Nat Immunol. 2003; 4:815. [PubMed: 12942076]

Kaye J, Hsu ML, Sauron ME, Jameson SC, Gascoigne NR, Hedrick SM. Selective development of CD4+ T cells in transgenic mice expressing a class II MHC-restricted antigen receptor. Nature. 1989; 341:746–749. [PubMed: 2571940]

Kobayashi T, Stang E, Fang KS, de Moerloose P, Parton RG, Gruenberg J. A lipid associated with the antiphospholipid syndrome regulates endosome structure and function. Nature. 1998; 392:193–197. [PubMed: 9515966]

Lee KH, Dinner AR, Tu C, Campi G, Raychaudhuri S, Varma R, Sims TN, Burack WR, Wu H, Wang J, et al. The immunological synapse balances T cell receptor signaling and degradation. Science. 2003; 302:1218–1222. Epub 2003 Sep 1225. [PubMed: 14512504]

Lee KH, Holdorf AD, Dustin ML, Chan AC, Allen PM, Shaw AS. T cell receptor signaling precedes immunological synapse formation. Science. 2002; 295:1539–1542. [PubMed: 11859198]

Li Q, Lau A, Morris TJ, Guo L, Fordyce CB, Stanley EF. A syntaxin 1, Galpha(o), and N-type calcium channel complex at a presynaptic nerve terminal: analysis by quantitative immunocolocalization. J Neurosci. 2004; 24:4070–4081. [PubMed: 15102922]

Martinez-Martin N, Risueno RM, Morreale A, Zaldivar I, Fernandez-Arenas E, Herranz F, Ortiz AR, Alarcon B. Cooperativity between T cell receptor complexes revealed by conformational mutants of CD3 epsilon. Sci Signal. 2009; 2:ra43. [PubMed: 19671929]

Monjas A, Alcover A, Alarcon B. Engaged and bystander T cell receptors are down-modulated by different endocytotic pathways. J Biol Chem. 2004; 279:55376–55384. Epub 52004 Oct 55328. [PubMed: 15516342]

Monks CR, Freiberg BA, Kupfer H, Sciaky N, Kupfer A. Three-dimensional segregation of supramolecular activation clusters in T cells. Nature. 1998; 395:82–86. [PubMed: 9738502]

Murphy GA, Graham SM, Morita S, Reks SE, Rogers-Graham K, Vojtek A, Kelley GG, Der CJ. Involvement of phosphatidylinositol 3-kinase, but not RalGDS, in TC21/R-Ras2-mediated transformation. J Biol Chem. 2002; 277:9966–9975. Epub 2002 Jan 9911. [PubMed: 11788587]

Niedergang F, Chavrier P. Regulation of phagocytosis by Rho GTPases. Curr Top Microbiol Immunol. 2005; 291:43–60. [PubMed: 15981459]

Niedergang F, Dautry-Varsat A, Alcover A. Peptide antigen or superantigen-induced down-regulation of TCRs involves both stimulated and unstimulated receptors. J Immunol. 1997; 159:1703–1710. [PubMed: 9257831]

Prieto-Sanchez RM, Berenjeno IM, Bustelo XR. Involvement of the Rho/Rac family member RhoG in caveolar endocytosis. Oncogene. 2006; 25:2961–2973. [PubMed: 16568096]

Rodriguez-Viciana P, Sabatier C, McCormick F. Signaling specificity by Ras family GTPases is determined by the full spectrum of effectors they regulate. Mol Cell Biol. 2004; 24:4943–4954. [PubMed: 15143186]

Rong R, He Q, Liu Y, Sheikh MS, Huang Y. TC21 mediates transformation and cell survival via activation of phosphatidylinositol 3-kinase/Akt and NF-kappaB signaling pathway. Oncogene. 2002; 21:1062–1070. [PubMed: 11850823]

Rosario M, Paterson HF, Marshall CJ. Activation of the Ral and phosphatidylinositol 3′ kinase signaling pathways by the ras-related protein TC21. Mol Cell Biol. 2001; 21:3750–3762. [PubMed: 11340168]

Saksena S, Sun J, Chu T, Emr SD. ESCRTing proteins in the endocytic pathway. Trends Biochem Sci. 2007; 32:561–573. Epub 2007 Nov 2007. [PubMed: 17988873]

San Jose E, Borroto A, Niedergang F, Alcover A, Alarcon B. Triggering the TCR complex causes the downregulation of nonengaged receptors by a signal transduction-dependent mechanism. Immunity. 2000; 12:161–170. [PubMed: 10714682]

Seminario MC, Bunnell SC. Signal initiation in T-cell receptor microclusters. Immunol Rev. 2008; 221:90–106. [PubMed: 18275477]

Sharma R, Sud N, Chattopadhyay TK, Ralhan R. TC21/R-Ras2 upregulation in esophageal tumorigenesis: potential diagnostic implications. Oncology. 2005; 69:10–18. Epub 2005 Jul 2028. [PubMed: 16088230]

Singleton K, Parvaze N, Dama KR, Chen KS, Jennings P, Purtic B, Sjaastad MD, Gilpin C, Davis MM, Wulfing C. A large T cell invagination with CD2 enrichment resets receptor engagement in the immunological synapse. J Immunol. 2006; 177:4402–4413. [PubMed: 16982875]

Smyth LA, Afzali B, Tsang J, Lombardi G, Lechler RI. Intercellular transfer of MHC and immunological molecules: molecular mechanisms and biological significance. Am J Transplant. 2007; 7:1442–1449. [PubMed: 17511673]

Swanson JA. Shaping cups into phagosomes and macropinosomes. Nat Rev Mol Cell Biol. 2008; 9:639–649. Epub 2008 Jul 2009. [PubMed: 18612320]

Umeshappa CS, Huang H, Xie Y, Wei Y, Mulligan SJ, Deng Y, Xiang J. CD4+ Th-APC with acquired peptide/MHC class I and II complexes stimulate type 1 helper CD4+ and central memory CD8+ T cell responses. J Immunol. 2009; 182:193–206. [PubMed: 19109150]

Vardhana S, Choudhuri K, Varma R, Dustin ML. Essential role of ubiquitin and TSG101 protein in formation and function of the central supramolecular activation cluster. Immunity. 32:531–540. [PubMed: 20399684]

Vigorito E, Bell S, Hebeis BJ, Reynolds H, McAdam S, Emson PC, McKenzie A, Turner M. Immunological function in mice lacking the Rac-related GTPase RhoG. Mol Cell Biol. 2004; 24:719–729. [PubMed: 14701744]

von Essen M, Nielsen MW, Bonefeld CM, Boding L, Larsen JM, Leitges M, Baier G, Odum N, Geisler C. Protein kinase C (PKC) alpha and PKC theta are the major PKC isotypes involved in TCR down-regulation. J Immunol. 2006; 176:7502–7510. [PubMed: 16751397]

Wetzel SA, Parker DC. MHC transfer from APC to T cells following antigen recognition. Crit Rev Immunol. 2006; 26:1–21. [PubMed: 16472066]

Yeung T, Grinstein S. Lipid signaling and the modulation of surface charge during phagocytosis. Immunol Rev. 2007; 219:17–36. [PubMed: 17850479]

Yokosuka T, Saito T. The immunological synapse, TCR microclusters, and T cell activation. Curr. 340:81–107.

Zerial M, McBride H. Rab proteins as membrane organizers. Nat Rev Mol Cell Biol. 2001; 2:107–117. [PubMed: 11252952]

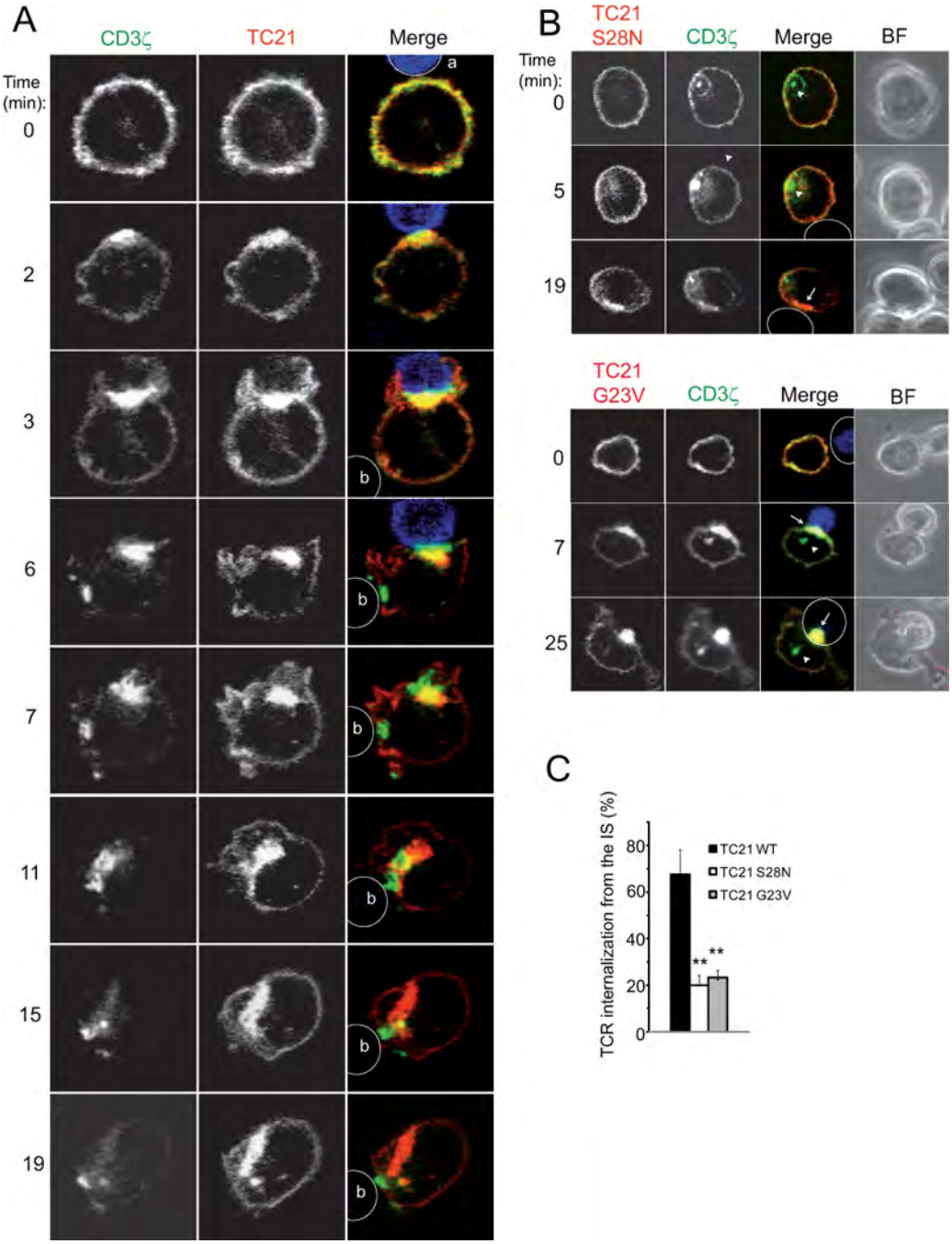

Figure 1.

The TCR is internalized from the IS by a TC21-dependent process. **(A)** TC21 is co-internalized with the TCR from the IS. Selected frames of images taken by time-lapse videomicroscopy of Jurkat cells transfected with CD3ζ-yellow fluorescent protein (YFP) and TC21-cyan fluorescent protein (CFP), and stimulated with SEE-loaded Raji APCs. The positions of two sequentially contacted APCs are indicated by circles in the merged images. For clarity, TC21-CFP emission is shown in red and CD3ζ-YFP in green. **(B)** Dominant negative and constitutively active forms of TC21 block TCR internalization from the IS.

Jurkat cells were transfected with CD3ζ-YFP and the indicated TC21 mutants (S28N: dominant negative; G23V: constitutively active). Arrows indicate the accumulation of the TC21 mutants and CD3ζ at the IS, while arrowheads indicate the existence of an intracellular pool of CD3ζ-YFP before stimulation (upper panel), and the emergence of a small pool of endocytic vesicles that contain CD3ζ but not TC21 (lower panel). The bright field (BF) image in the lower panel shows the formation of extensive membrane protrusions by the T cell at the T cell:APC contact area (red dots). **(C)** Quantification of TC21 mutant effect on CD3ζ internalization from the IS. A number of 15-20 single T:B cell conjugates were scored according to the presence of CD3ζ in vesicles immediately below the IS. Each value represents the mean and standard deviation of three datasets.$^{**}P < 0.005$ (two-tailed Mann-Whitney test).

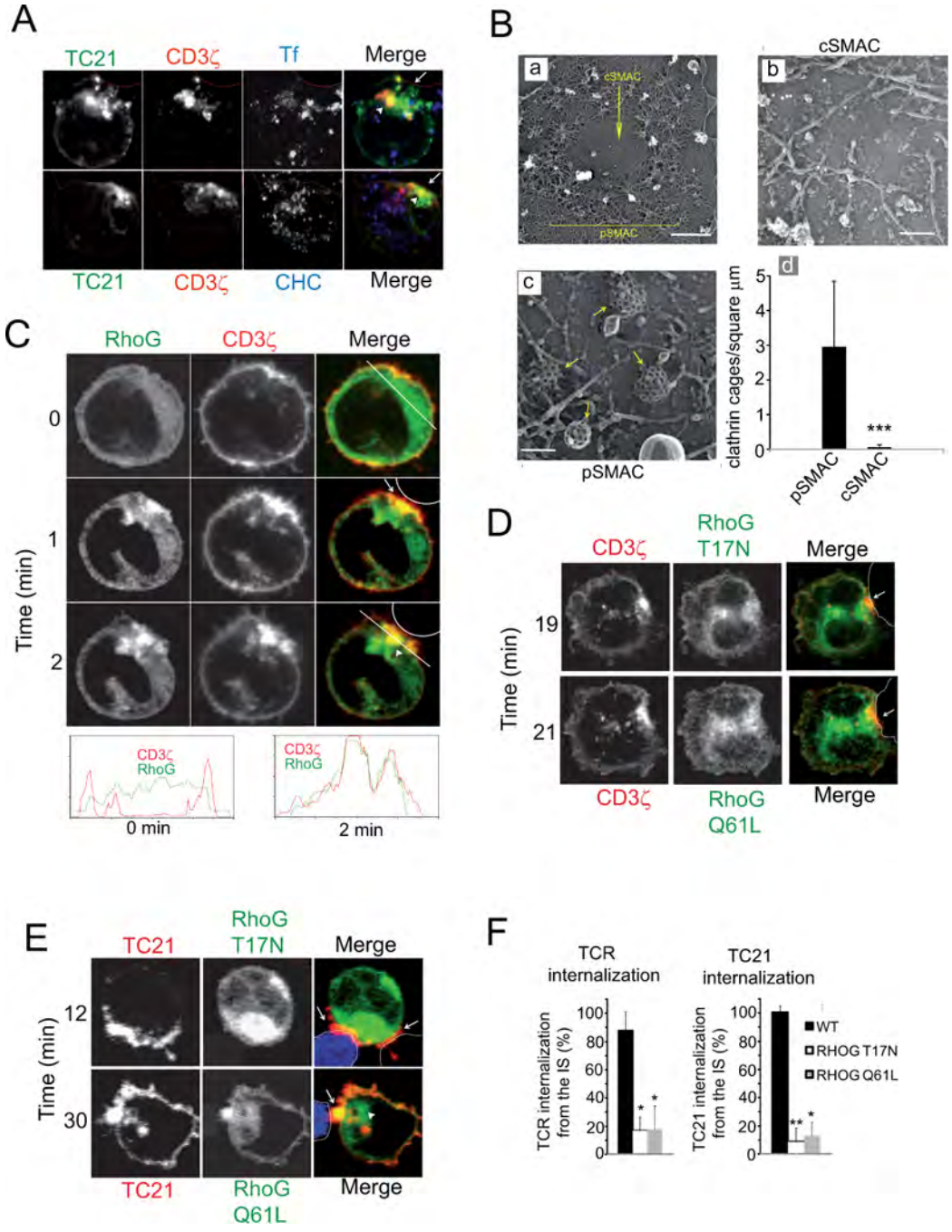

Figure 2.

The TC21-dependent mechanism of TCR internalization is RhoG-dependent but independent of clathrin. **(A)** TCR and TC21 double positive endocytic vesicles are negative for markers of clathrin-dependent endocytosis. Jurkat cells transfected with CD3ζ-Cherry and TC21-GFP were stimulated with SEE-loaded Raji for 30 min and were either incubated with Alexa633-labeled transferrin during the last 5 minutes (upper panels) before fixation or stained with anti-clathrin heavy chain (CHC; lower panels). Arrows indicate the position of the IS and arrowheads internal vesicles double positive for TC21 and CD3ζ. The images are

representative of 50 cells examined per condition. **(B)** The cSMAC is devoid of coated pits. Primary naïve mouse T cells were plated on patterned arrays containing a central anti-CD3 spot surrounded by ICAM-1. Cells were unroofed and prepared for freeze-etch electron microscopy. A typical pattern with actin rings surrounding a central bare spot was seen (micrograph a, scale bar-1 μm). More vigorous sonication removed the actin ring revealing large numbers of clathrin cages in the pSMAC (yellow arrows, micrograph c, scale bar-100 nm) but not in the cSMAC (micrograph b, scale bar-100 nm). Quantification of the number of clathrin cages in the pSMAC vs. cSMAC areas was performed from a series of 17 photographs corresponding to the pSMAC and 3 photographs to the cSMAC and expressed in d as number of cages per square micrometer. ***$P < 0.0005$ (two-tailed Mann-Whitney test). Scale bars **(C)** TCR is internalized from the IS in RhoG-positive vesicles. Jurkat cells were transfected with both wild type RhoG-GFP and wild type CD3ζ-Cherry, and they were stimulated with SEE-loaded Raji for the times indicated. The Raji APCs are encircled in the merged images. The arrow indicates the accumulation of TCR at the IS, while the arrowhead indicate the presence of IS-derived vesicles containing TCR that are positive for RhoG. ICA of RhoG and CD3ζ across the section indicated with a white line at times 0 and 2 min in the merged images are shown at the bottom to illustrate how RhoG concentrates in CD3ζ-positive vesicles. **(D)** Both the dominant negative and constitutively active RhoG mutants block TCR internalization from the IS. Jurkat cells transfected with CD3ζ-Cherry and either dominant negative (T17N) or constitutively active (Q61L) mutants of RhoG-GFP were stimulated for the times indicated. The arrows indicate the presence of TC21 at the IS. **(E)** Both dominant negative and constitutively active RhoG mutants block TC21 internalization from the IS. Jurkat cells transfected with wild type TC21-DsRed, and either the T17N or the Q61L mutants of RhoG-GFP, were stimulated for the times indicated. The presence of TC21 at the IS is indicated by arrows, while the presence of RhoG-positive, TC21-negative internal vesicles is indicated by arrowheads. **(F)** Quantification of the effect of RhoG mutants on CD3ζ and TC21 internalization from the IS. 15–20 single T:B cell conjugates were scored according to the presence of either CD3ζ or RhoG in vesicles immediately below the IS. Each value represents the mean and standard deviation of three datasets. *$P < 0.05$, and **$P < 0.005$ (two-tailed Mann-Whitney test).

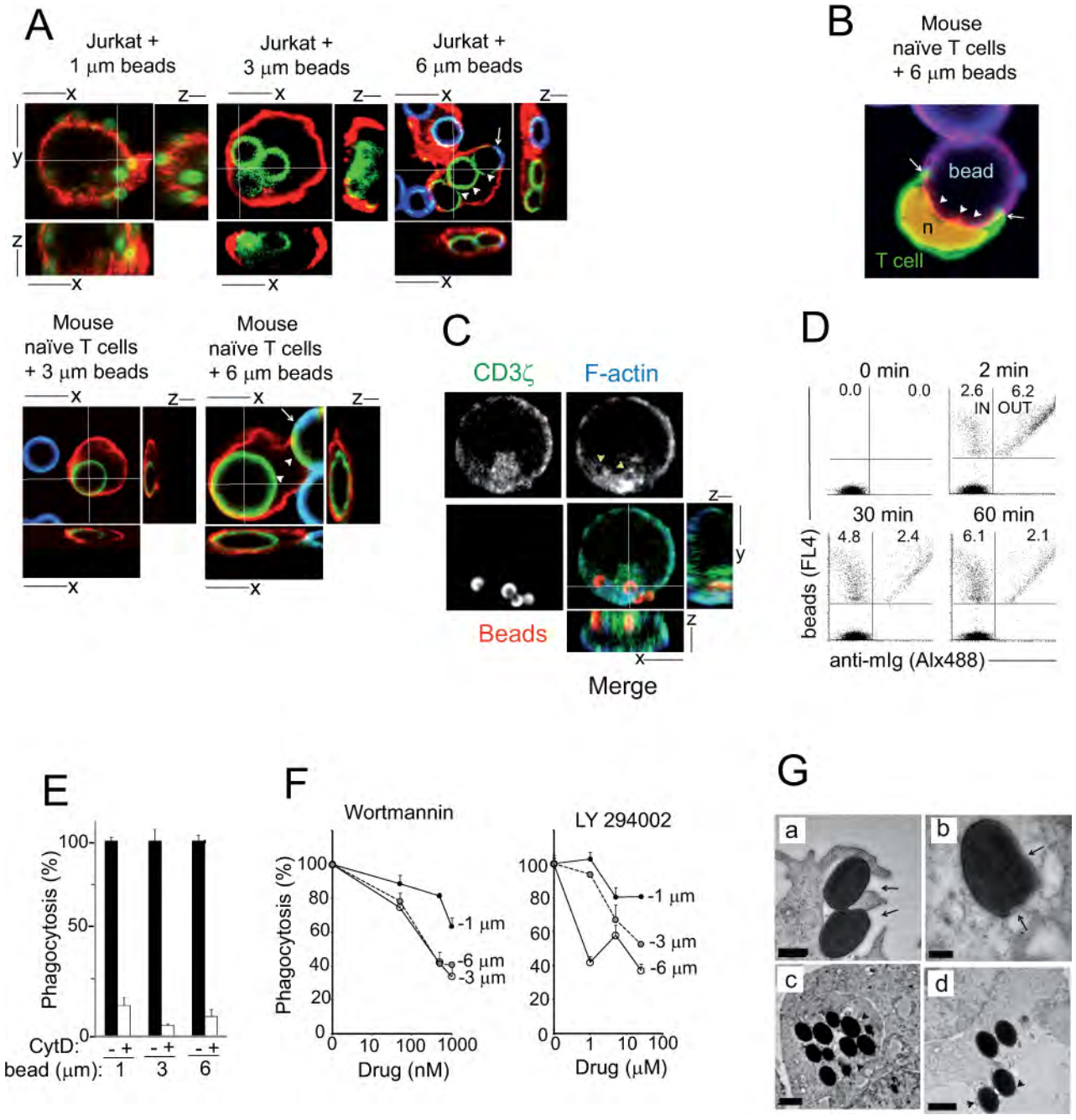

Figure 3.

TCR-triggered phagocytosis. **(A)** T cells phagocytose anti-CD3-coated latex beads. Jurkat and primary mouse naïve T cells were incubated with 1–6 μm diameter fluorescent beads (shown in green) for 30 min and stained with fluorescent phalloidin to visualize the cortical F-actin (in red). Optical sections along the xy, yz and xz axis are shown to demonstrate that some beads are completely internalized. A secondary Alexa 647-labeled anti-mouse Ig (shown in blue) was added to determine if the 3 μm and 6 μm antibody-coated beads were accessible or not. This distinguished fully internalized (arrowheads) from external beads, and even detected phagocytotic cups (arrows) in which the bead is partly inaccessible to the

secondary antibody. **(B)** T cells form a tight seal in the phagocytotic cup. Naïve mouse cells stimulated for 30 min with anti-CD3 coated 6 μm beads were fixed, permeabilized and stained with phalloidin-TRITC (shown in green), To-Pro to visualize the nucleus (n, orange), and with an Alexa 488-labeled secondary anti-hamster Ig antibody (shown in blue) to distinguish internal from non-phagocytosed beads. Arrows indicate a tight apposition of the actin cytoskeleton to the bead at the growing edges of the phagocytotic cup. Arrowheads indicate the part of the bead facing the cell that is not accessible to the anti-Ig antibody and that therefore, is red but not blue. **(C)** Phagocytosed beads are associated with both the TCR and polymerized actin. Human primary T cell lymphoblasts were incubated with anti-CD3-coated 1 μm beads for 60 min and stained with with phalloidin and an anti-CD3ζ antibody to visualize the endogenous TCR. Arrowheads indicate the presence of polymerized actin around the phagocytosed beads. **(D)** Quantitative assay of bead phagocytosis. Jurkat cells were incubated at 37°C with red fluorescent 1 μm beads coated with anti-CD3 for the times indicated and subsequently, with a secondary Alexa 488 anti-Ig antibody at 0°C. **(E)** TCR-triggered phagocytosis is dependent on the actin cytoskeleton. Jurkat cells were incubated for 30 min with either 1, 3 or 6 μm anti-CD3-coated beads in the presence or absence of 1 μg/ml cytochalasin D (CytD). The percentage of phagocytosis was calculated according to the in/out ratio as shown in panel D. Each value represents the mean and standard deviation of three datasets. **(F)** Particle size and PI3K-dependence. Jurkat T cells pre-incubated with the indicated inhibitors were incubated with 1–6 μm anti-CD3-coated beads for 30 min and phagocytosis was assessed as in panel D. Each value represents the mean and standard deviation of three datasets. **(G)** Partially and totally phagocytosed beads are tightly surrounded by membranes. Jurkat cells were incubated with 1 μm anti-CD3-coated beads for 5 (a), 15 (b), 30 (c) or 60 min (d), and they were prepared for transmission electron microscopy. Arrows indicate the presence of a phagocytic cup in micrograph a, and the presence of membranes around phagocytosed beads in b. Arrowheads indicate the presence of membrane vesicles in what appears a multivesicular body in c and of particles associated to egressing beads in d. Scale bars: 500 nm (a), 200 nm (b), 1 μm (c and d)

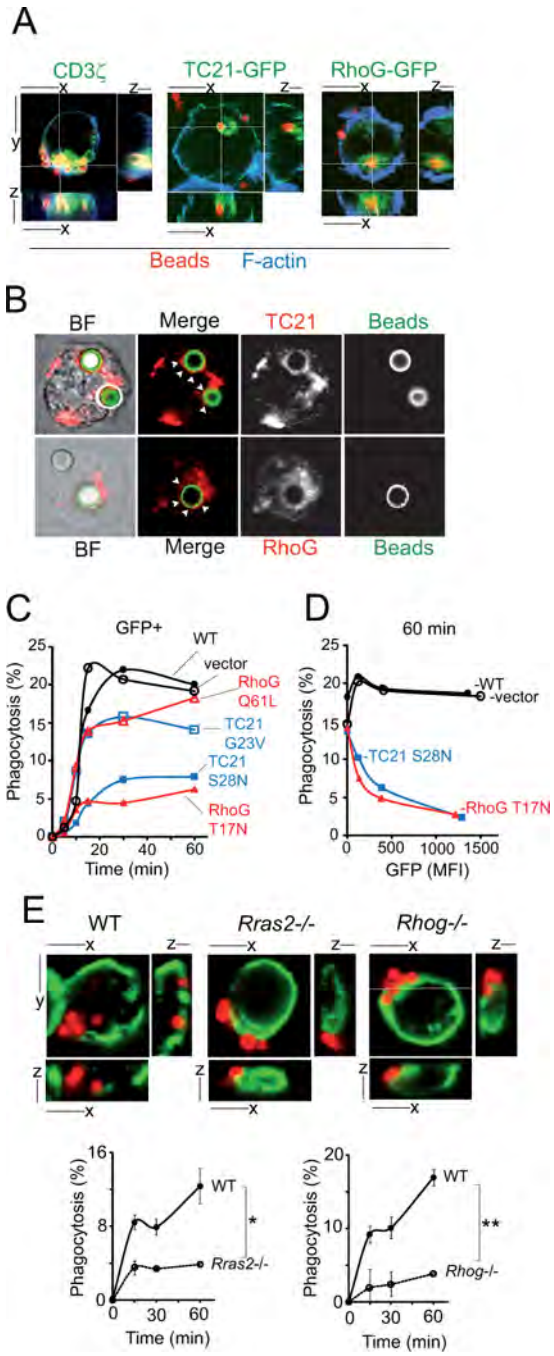

Figure 4.

TCR-triggered phagocytosis requires TC21 and RhoG activities. **(A)** Phagocytosed beads are associated to the TCR, TC21 and RhoG. Jurkat cells were transfected with TC21-GFP or RhoG-GFP and they were incubated for 60 min with fluorescent 1 μm anti-CD3 coated beads. Untransfected Jurkat cells were incubated with beads in the same conditions and the endogenous TCR was visualized with a CD3ζ antibody. **(B)** Phagocytosed beads are associated with endogenous proteins. Untransfected Jurkat cells were incubated with 3 μm anti-CD3 coated green beads for 30 min and stained with either anti-TC21 or anti-RhoG. **(C)**

TCR-triggered phagocytosis is TC21- and RhoG-dependent. Jurkat cells were transfected with the constructs indicated, incubated with fluorescent anti-CD3-coated beads and phagocytosis was analyzed as in Fig. 3D. WT, cells transfected with wild type TC21-GFP; vector, cells transfected with the empty vector. **(D)** Dose dependency of the effect of mutant TC21 and RhoG. The efficiency of phagocytosis is shown as a function of the amount of GFP fusion protein. **(E)** TCR-triggered phagocytosis is impaired in T cells genetically deficient in TC21 or RhoG. Lymph node T cells of the indicated genotypes that were stimulated for 60 min with anti-CD3-coated 1μm red fluorescent latex beads were examined by confocal microscopy after staining with phalloidin (green). In parallel, phagocytosis was quantified by flow cytometry (as in Fig. 3D) at the times indicated (bottom). Each value represents the mean and standard deviation of three datasets. *$P < 0.05$, and **$P < 0.005$ (two-tailed Mann-Whitney test).

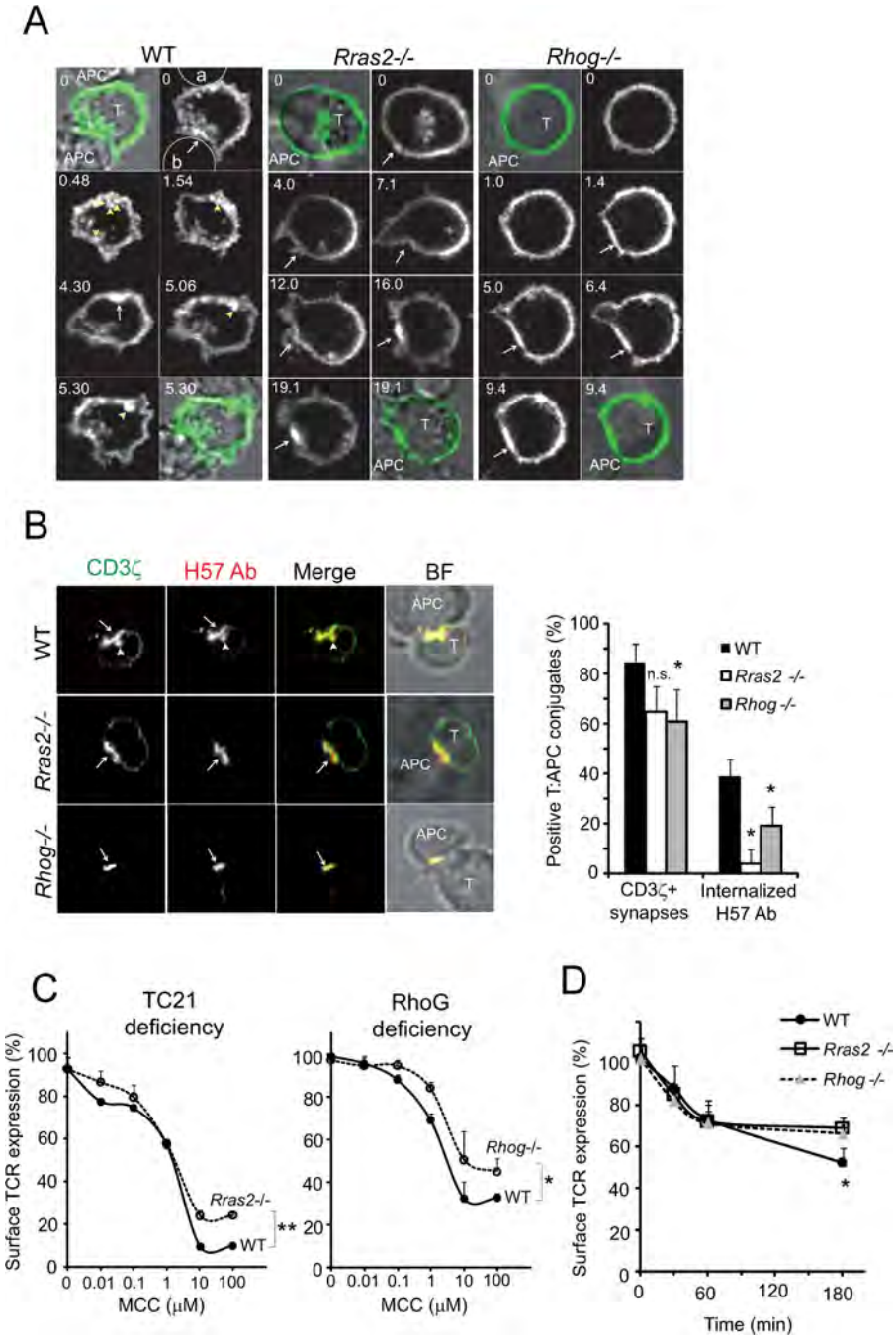

Figure 5.

The TCR is internalized from the IS by a TC21- and RhoG-dependent mechanism. **(A)** The TCR is retained at the IS in the absence of TC21 or RhoG. Lymph node T cells from AND TCR transgenic mice with the indicated genotypes were transduced with a CD3ζ-GFP lentivirus and stimulated with MCC peptide antigen-loaded DCEK cells as APCs. Formation of the IS and TCR internalization from the IS was followed by time-lapse videomicroscopy according to the distribution of CD3ζ-GFP. Arrows indicate the accumulation of CD3ζ-GFP at the IS. The WT T cell makes two ISs, first with APC b and later with APC a. The

emergence of internal vesicles derived from both ISs is indicated with yellow arrowheads. **(B)** Quantification of TCR internalization from the IS. For quantification, AND T cells were stained on ice with the anti-TCRβ antibody H57-597 (H57) before they were stimulated for 30 min with MCC-loaded DCEK. The formation of an IS was quantified according to the percentage of T:APC cell conjugates with CD3ζ concentrated at the synapse. The internalization of the TCR from the IS was quantified according to the percentage of T cells with internal vesicles positive for both the anti-CD3ζ and H57 antibodies. Arrows indicate the position of the IS and arrowheads the presence of endocytic vesicles containing TCR that have been internalized from the IS. A total of 20–30 conjugates per genotype were studied in triplicate (right panel). *$P < 0.05$ (two-tailed Mann-Whitney test); n.s, not significant. **(C&D)** TC21 and RhoG deficiencies have a weak effect on TCR downregulation. AND T cells of the indicated genotype were stimulated for 3 hr with DCEK cells loaded with the indicated concentrations of MCC peptide (C) or for the times indicated with DCEK loaded with 100 μM MCC (D). TCR downregulation was calculated according to the mean fluorescence intensity of the AND TCR with an anti-Vβ3 antibody. Each value represents the mean and standard deviation of three datasets. *$P < 0.05$, and **$P < 0.005$ (two-tailed Mann-Whitney test).

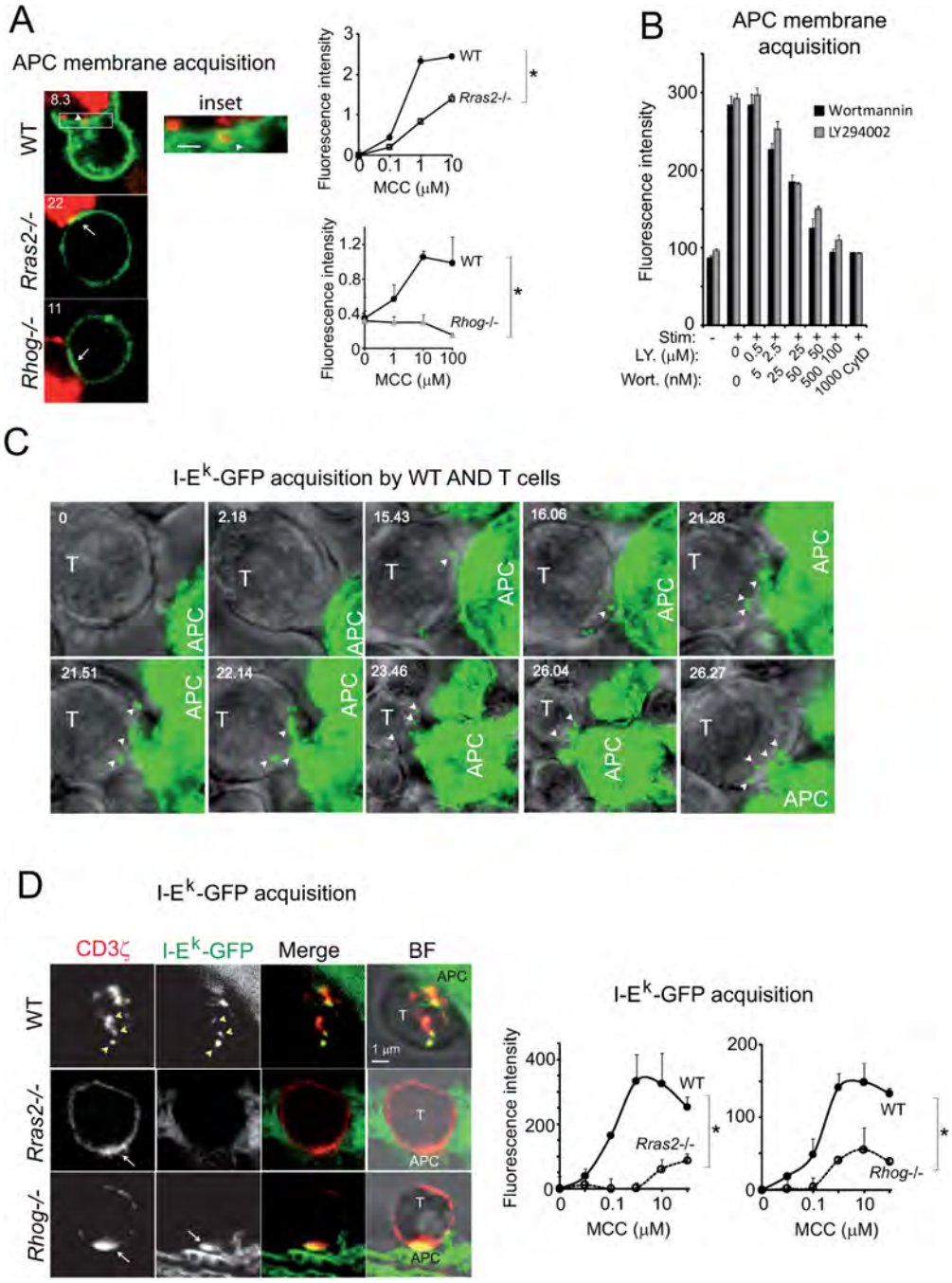

Figure 6.

TC21 and RhoG mediate trogocytosis and the uptake of MHC class II by T cells. **(A)** TC21 and RhoG mediate TCR-induced trogocytosis of APC membrane fragments. AND lymph node T cells of the indicated genotypes were transduced with CD3ζ-GFP and stimulated with MCC-loaded DCEK cells previously labeled with the red fluorescent dye PKH26. Conjugate formation was recorded by time-lapse videomicroscopy. The arrows indicate the formation of an IS and the arrowhead the presence of an endocytotic vesicle containing fragments of the red-labeled APC membrane. The inset shows a magnification of the T

cell:APC contact area of the wild type T cell 8.3 min after stimulation (scale bar-1μm). Quantification of PKH26 uptake by the T cells (right) was performed by flow cytometry after gating of $CD4^+$ T cells. Each value represents the mean and standard deviation of three datasets. *$P < 0.05$ (two-tailed Mann-Whitney test). **(B)** Trogoctyosis of APC membrane fragments is PI3K-dependent. Wild type AND lymph node T cells were stimulated with MCC-loaded (+) or unloaded (-) DCEK cells previously labeled with the red fluorescent dye PKH26 in the presence of the indicated concentrations of either wortmanin or LY294002 PI3K inhibitors. APC membrane acquisition by the T cell was quantified by flow cytometry according to the acquisition of PKH26 label by the T cells. CytD indicates cells stimulated in the presence of 1 μg/ml cytochalasin D. **(C)** T cells take up MHC class II from APCs from the IS. DCEK cells were transiently transfected with the I-Eα^k-GFP construct and incubated with unlabeled purified naïve wild type AND T cells and recorded by time-lapse videomicroscopy. Arrowheads indicate the presence of vesicles in the T cell containing I-Eα^k-GFP that have been acquired from the IS. **(D)** T cells take up MHC class II from APCs by a TC21 and RhoG-dependent mechanism. DCEK cells were transiently transfected with the I-Eα^k-GFP construct and incubated with AND T cells of the indicated genotype. The formation of IS was visualized after staining with anti-CD3ζ. Yellow arrowheads show IS-derived vesicles that contain both the TCR (CD3ζ) and I-Eα^k-GFP acquired from the APC. Arrows indicate the accumulation of CD3ζ at the IS of *Rras2*$^{-/-}$ and *Rhog*$^{-/-}$ mice. In the RhoG-deficient T cell, I-Eα^k-GFP also accumulates at the IS but it is not trogocytosed by the T cell. Quantification of I-Eα^k-GFP uptake by the T cells (right) was performed by flow cytometry after gating on $CD4^+$ T cells. Each value represents the mean and standard deviation of three datasets. *$P < 0.05$ (two-tailed Mann-Whitney test).

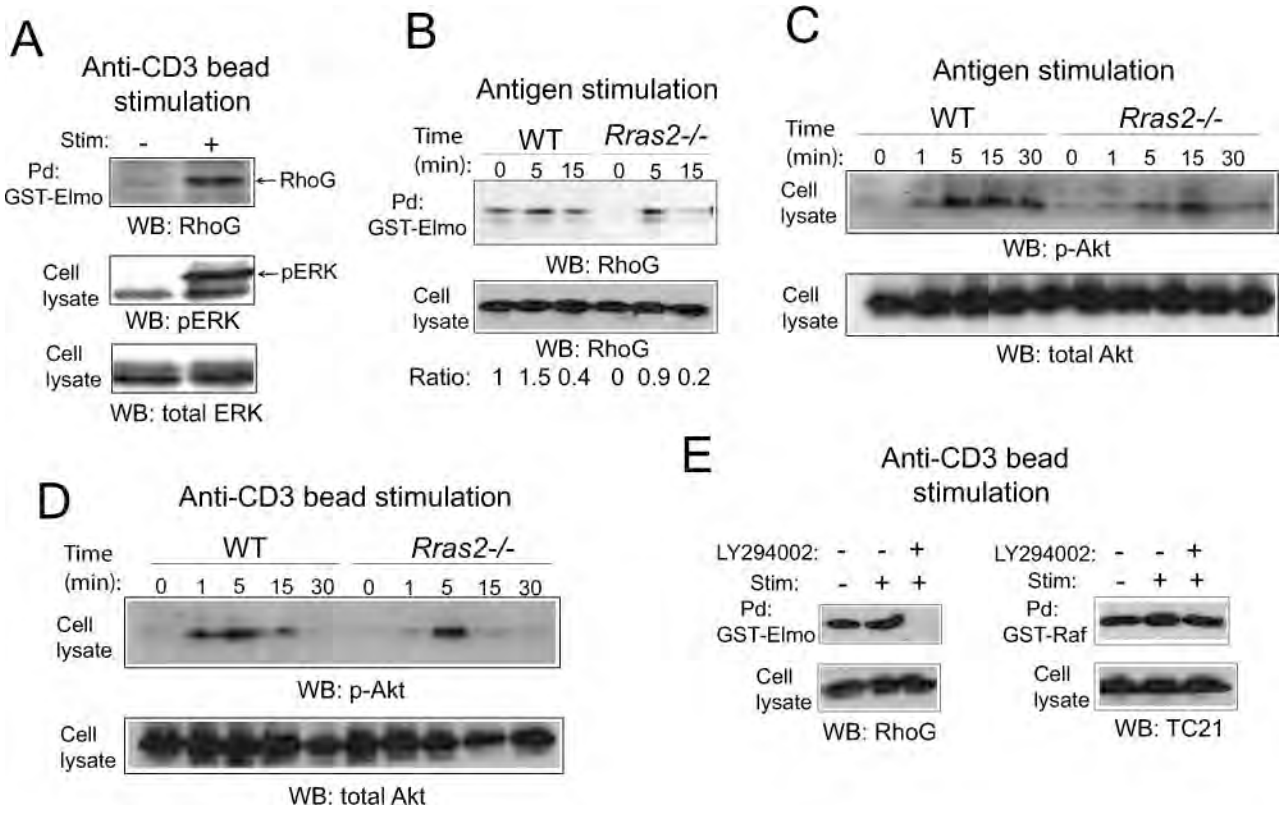

Figure 7.

RhoG is activated by the TCR via a TC21 and PI3K-dependent pathway. **(A)** TCR triggering with immobilized anti-CD3 antibody activates RhoG. Jurkat cells were stimulated for 2 min with anti-CD3-coated 1 m beads (40:1 bead/cell ratio). Pull-down (Pd) with GST-ELMO was performed on cell lysates that were then analyzed in western blots (WB) probed with anti-RhoG to estimate RhoG activity. WB probed with anti-phosphoERK and total ERK antibodies were performed as controls of activation and loading, respectively. **(B)** Antigen stimulated activation of RhoG is TC21-dependent. AND T cells of the different genotypes were incubated for the times indicated with DCEK APCs preloaded with 10 μM MCC. Pull-down with GST-ELMO was used to isolate active RhoG. WB probed with anti-RhoG from whole cell lysates were used as a loading control. Quantification was carried out by densitometry and dividing the intensity of the bands in the GST-ELMO pull-down by those of the whole cell lysates. Comparison of the resulting values was performed by dividing them by this of the WT cells at time 0, that was considered as 1. **(C&D)** TCR-triggered phosphorylation of Akt is TC21-dependent. AND T cells of the indicated genotypes were incubated with DCEK APCs preloaded with 10 μM MCC (C) or stimulated with anti-CD3 coated 1 μm beads (D) for the times indicated. WB were probed with anti-phosphoAkt antibody of whole cell lysates as an indication of PI3K activity. **(E)** RhoG activation but not TC21 activation is PI3K dependent. Wild type T cell lymphoblasts were stimulated with anti-CD3 coated 1 μm beads for 5 min in the presence or absence of 50 μM LY294002 PI3K inhibitor. Pull-down with GST-ELMO was used to isolate active RhoG and pull-down with GST-Raf1(RBD) to isolate active TC21. Whole cell lysates were used as loading controls.